Simple and complex multidimensional actomyosin crossbridges

C Dave, Mikey R, Tommy D

2009 - 06 - 25

Abstract

The 4 spring crossbridge (4sXB) is able to accurately model the movements believed to be behind the generation of force by myosin during the power stroke. The 2 spring crossbridge (2sXB) shares many of the desirable properties of the 4sXB, such as the elimination of linear offsets in favor of experimentally measured changes in lever angle. Both the 4sXB and the 2sXB maintain similar kinetics to previous work at resting lattice spacings, permitting more direct comparison of work done with either system to previous studies. Unlike the 4sXB, the length and angle of the springs comprising the 2sXB can be analytically determined for any chosen head position without the use of iterative techniques. Both the 4sXB and the 2sXB are able to measure the radial forces generated by during the production of axial force. Similarly, both proposed crossbridge systems take lattice spacing into account in every aspect of their operation. Lattice spacing dependent kinetics are derived based on the work of Pate and Cooke. Lattice spacing dependent axial and radial forces are measured and considered.

Currently, abstract gives main points of the paper.

Keywords: myosin; spatially-explicit model; crossbridge kinetics

Author Summary Models of muscle contraction have long treated the molecular motor myosin as a simple spring oriented parallel to its direction of movement. This does not allow for the investigation of phenomena such as the perpendicular force observed during shortening, or the dependence of the maximum force produced on spacing between the contractile filaments that comprise muscle. We demonstrate an alternative model, computationally simple enough to use in large networked models, that incorporate both linear and torsional or angular springs. These models capture much of the behavior missing from previous efforts.

1 Introduction

Needs a purpose and a rewrite.

Sarcomere-scale modeling of muscle contraction has changed since the introduction of the sliding crossbridge model in the 1950s, but the geometry of the individual crossbridges used has remained largely unaltered. While individual crossbridges have been treated independently with spatial modeling, thermodynamic accounting has been introduced to the crossbridge kinetics, compliance introduced to the filaments, and multiple filaments have been arranged to mimic the lattice, the one dimensional nature of the crossbridge has continued to be used as a model of the mechanism of force generation. We propose that with a shift to crossbridges that use two or four four springs, new insight into the effects of lattice spacing and radial forces generated during axial shortening may be gained.

The now-traditional single spring crossbridge introduced by Huxley (1) has been the dominant model used in modeling studies since its introduction. The geometry of the single spring crossbridge has remained largely unchanged while the kinetics underlying transitions between force generating states have been increased in complexity throughout subsequent work. (2–5) Meanwhile, Houdusse and Sweeney (6) and others have proposed that the region of the lever arm directly adjacent to the converter region is a flexible area that acts as a spring. This model of force generation by myosin suggests that inclusion of torsional spring might create a system that better reflects the underling mechanisms of the powerstroke.

We propose and compare two torsional spring based crossbridge models that are targeted for use in spatially explicit models of the half sarcomere. The first is a four spring crossbridge (4sXB) that is directly inspired by the structure of the S1 and S2 regions of myosin II. Following this, we consider a two spring crossbridge (2sXB) that replicates many of the behaviors of the 4sXB while requiring fewer computational resources.

This discussion owes a debt to Schoenberg (7) and Schoenberg (8) which contain a proposal and analysis of several different types of crossbridges, primarily two spring crossbridges where the S2 arm is represented as a linear spring and the S2-S1 junction area is represented as a torsional spring. This system requires iterative solution methods, as our four spring crossbridge does, but restrains the crossbridge to an area within one S1 length of the line in which the S2 segment is set.

2 Materials and Methods

We restrict our analysis to representations of crossbridges that are useful for spatially explicit modeling of the half-sarcomere, i.e. models utilizing from one to several springs. Representations of the crossbridge as a single spring have been used extensively in previous work and serve as a baseline against which we can compare more complicated models. A crossbridge comprised of four springs is able to replicate both the known geometry of the crossbridge and the movements that comprise the power stroke. A simpler crossbridge consisting of just two springs, able to replicate most of the four spring crossbridge's behavior, is also described.

Geometry

Spring configurations The 1sXB consists of a single linear spring aligned parallel to the thick and thin filaments. As described above, it is insensitive to changes in lattice spacing and is unable to account for radial forces generated during axial shortening.

The 4sXB uses two linear and two torsional springs to represent the myosin head, as depicted in Fig 5D. This allows the springs used in the model to closely correspond to pieces of the crossbridge. Specifically the four springs correspond to the S2 attachment region, the lever arm, the pliant region/converter domain, and the globular head region. Additionally, the additional springs of the 4sXB cause it to occupy two dimensions, where the 1sXB only occupies one. This two dimensionality allows the 4sXB to be embedded in a space that takes the distance between thick and thin filaments into account, introducing lattice spacing dependence.

The 2sXB uses one linear and one torsional spring to represent the myosin head, as depicted in Figure 5C. This crossbridge acts as a simplification of the 4sXB, retaining movement generated by a lever arm, but altering the length of the lever such that it can bridge the entire distance between the thick and thin filaments. The parameters characterizing the 2sXB are chosen to match the step size and kinetics of the 2sXB to those of the 4sXB.

Each type of crossbridge has several physical parameters that must be set before they may be used. Each linear spring (one in the 1sXB, two in the 4sXB and one in the 2sXB) requires a rest length and spring constant, while each torsional spring (two in the 4sXB and one in the 2sXB) requires a rest angle and spring constant. The rest length or angle of one spring in each crossbridge is altered during the transition from a weakly bound state to a strongly bound state, in order to produce the force that tensions the linked filaments.

Displacement and force generation The geometry of the 1sXB model of the crossbridge has evolved with an eye towards accounting for the offset generated by the powerstroke and the energy utilized in the creation of this offset. From these two concerns the force the spring (assuming it to be a linear one) can produce is accounted for. In a two dimensional model there is the additional goal of replicating the crossbridge's sensitivity to lattice spacing and multidimensional force generated.

Calculation of spring lengths and angles When the 1sXB is distorted such that the myosin head is horizontally offset from thick filament attachment site relative to its resting position, the length of the 1sXB's spring is simple to find as it must completely span the head to thick filament attachment distance. The lengths and angles of the springs in the 2sXB and 4sXB must take into account the radial distance they must cover as well, but remain simple to calculate. The 2sXB may be analytically determined, as it has all spring values set by the choice of a head location, with arm length and angle given by $r(h_x, h_y) = (h_x^2 + h_y^2)^{1/2}$ and $\theta(h_x, h_y) = \arctan(h_y/h_x)$, respectively. The 4sXB suffers from increased computational complexity over the 1sXB and 2sXB systems in that iterative optimization is required to find the location of the distal torsional spring representing the converter region when the crossbridge's head is moved to a new location. We use a modification of Powell's "dog-leg" method[1] to relax the location of the distal torsional spring to that which results in the lowest energy state of the 4sXB. Once the distal torsional spring's location is known (as (c_x, c_y)), the angle of the proximal torsional spring and the lengths of the two linear springs are analytically determinable. The angle of the proximal torsional spring is given as $\phi(c_x, c_y) = \arctan(c_y/c_x)$, the length of the proximal linear spring as $\ell(c_x, c_y) = (c_x^2 + c_y^2)^{1/2}$, the angle of the distal torsional spring as $\theta(c_x, c_y, h_x, h_y) = \arctan((h_y - c_y)/(h_x - c_x)) + \pi - \phi(c_x, c_y)$, and the length of the distal linear spring as $r(c_x, c_y, h_x, h_y) = ((h_x - c_x)^2 + (h_y - c_y)^2)$.

Kinetics

As in other recent works, such as Tanner et al. (5), we choose to use a simplified three state model of the crossbridge cycle with energies based on the work of Pate and Cooke in Pate and Cooke (2). This simplified system allows for the most direct linking of the crossbridge's kinetics and chemo-mechanics; the three kinetic states being directly comparable to the myosin configurations described in Houdusse et al. (9). A secondary benefit of a three state kinetics system is that it allows multiple-motor models which use our many-spring crossbridges to more easily compare their results to those from the aforementioned previous models.

[1] Present in the SciPy package of computational tools.

The three states represented in our kinetics are an unbound state, a loosely-bound state, and a tightly-bound force-generating state. As depicted in figure 5 A, these states correspond to a Myosin-ADP-Pi state, an Actin-Myosin-ADP-Pi state, and an Actin-Myosin-ADP state.

The kinetics of both the two spring and the four spring models are strain dependent and are essentially transforms of the free energy landscapes experienced by the crossbridges in their different states. These free energies are a function of the distortion necessary to move the point representing the crossbridge's head to the point where we presume a binding site to be. Examples of these free energy landscapes are visible in figures 5A and 5B, with cuts through them at the rest lattice spacing visible in figure 5A.

The binding of both the two and four spring crossbridges is determined by Monte-Carlo simulation of their diffusion as a result of being perturbed by Boltzmann derived energy distributions. After a new head location is found, a binding probability is calculated that decreases exponentially with distance from the potential binding site. This probability is tested against a random number from a uniform distribution to determine if binding occurs.

Free energy in each state The total energy, liberated by the hydrolysis of a P_i, available to a crossbridge is dependent on the concentrations of ATP, ADP and P_i in the system and is given by $\Delta G = -\Delta G_{0,ATP} - \ln \frac{[ATP]}{[ADP][P_i]}$. In the weakly bound and strongly bound states a portion of that energy has been made available to the crossbridge, allowing the crossbridge in the latter two states to convert at most 28% or 68% of ΔG into useable work respectively. (2, 5) These efficiency factors are used as $\alpha = 0.28$ and $\eta = 0.68$ below. The free energy of a crossbridge in each state it a function of both the energy available as described above and the strain that the crossbridge is currently experiencing as a result of post-binding distortion. Combining the distortion dependence and liberated energy terms gives us the total free energy of the crossbridge in each state. The free energy of the 4sXB system in each state is:

$$\begin{aligned}
U_1(\phi,\ell,\theta,r) &= 0 \\
U_2(\phi,\ell,\theta,r) &= \alpha\Delta G + \frac{k_\phi(\phi-\phi_0)^2 + k_\ell(\ell-\ell_0)^2 + k_\theta(\theta-\theta_0)^2 + k_r(r-r_0)^2}{2} \\
U_3(\phi,\ell,\theta,r) &= \eta\Delta G + \frac{k_\phi(\phi-\phi_0)^2 + k_\ell(\ell-\ell_0)^2 + k_\theta(\theta-\theta_1)^2 + k_r(r-r_0)^2}{2}
\end{aligned}$$

The free energy of the 2sXB system in each state is:

$$\begin{aligned}
U_1(r,\theta) &= 0 \\
U_2(r,\theta) &= \alpha\Delta G + \frac{k_r(r-r_0)^2 + k_\theta(\theta-\theta_0)^2}{2} \\
U_3(r,\theta) &= \eta\Delta G + \frac{k_r(r-r_1)^2 + k_\theta(\theta-\theta_1)^2}{2}
\end{aligned}$$

Calculation of binding rate Our binding rates are a determined by thermally forcing unattached heads to a diffused location and then applying a probability of attachment that is an exponential function of the distance from the diffused location to the nearest available actin site. The thermal forcing of the unattached heads take the form of choosing an offset from a Boltzman distribution for each of the head's constituent springs, finding their resulting lengths and angles, and then using those values to determine the new head location. The PDF of the an offset location is given by $P(x) = \sqrt{k/(2\pi kT)}\exp^{-(kx^2)/(2kT)}$ where x is the offset, k is the spring constant of the spring in question, and T is the system's temperature. Once the offset of each spring is determined, the new head location can be determined from the spring system's geometry and the distance to the binding site found. Myosin binding is determined to be a exponential function of the distance ($dist$) from the myosin head to the available binding site, such that the probability of the binding is given by $r_{12}(dist) = \gamma \exp^{dist}$, where γ is a scaling factor. Such a system is very computationally efficient in use, but binding rates as a function of myosin head starting location (as opposed to head to binding stie distance) must be computed by approximation as a fraction of n binding opportunities, using a newly diffused head location and checking against a random number $rand$, ranging from zero to one, which is generated for each trial thus: $r_{12} = (\sum^n (1 \text{ if } \gamma \exp^{-(\text{post diffusion distance})} > rand, \text{ else } 0))/n$. This is applied uniformly to the 4sXB and the 2sXB, with the only difference being the number of springs subject to thermal forcing in each instance.

Powerstroke and detachment rates The rate of transition from a weakly bound state to a strongly bound one and the rate of detachment from a strongly bound state are distortion dependent and based on the earlier work of Pate and Cooke (2) and Tanner et al. (5), but generalized to be useable by the 4sXB and 2xB in two-dimensional space. Distortion dependence is introduced into the r_{23} and r_{31} rates as a term based on the differences in free energy between the current state and the one being considered for transition. This means that transitions are more likely when they are energetically favorable and less likely in other circumstances, a natural scheme based in the geometry of the crossbridges. The particular rates are as follows for both the 4sXB and the 2sXB:

$$r_{23}(U_2, U_3) = 0.001 + 0.5 * (1 + \tanh(0.6(U_2 - U_3)))$$

$$r_{31}(U_3, U_1) = e^{-1/(U_3 - U_1)}$$

Calculation of reverse rates The rates of transitions in the direction opposite from those described above, e.g. from strongly to weakly bound or from a weakly bound state to an unbound state, are given by the thermodynamically balancing formula $r_{ij}/r_{ji} = \exp^{U_i - U_j}$ where r_{ij} is the reverse rate and r_{ji} is the forward rate. For the transition from a weakly bound state to an unbound state

this requires that the reverse transition is again treated as a fraction of a sum of n transition opportunities.

3 Results

The consequence of using the proposed multi-spring crossbridges include the introduction of sensitivity to lattice spacing in the kinetics and force that respectively govern and are generated by the crossbridge head. The 4sXB and 2sXB's properties most commonly display one of two lattice spacing sensitivities: alteration of the baseline values or offset of key points in the profile of a value. Baseline value changes occur where the lowest points, the highest points, or simply the offset of a value is shifted with regard to that seen at rest lattice spacing. Baseline value changes manifest in, e.g./, the lowered probability of any binding occurring at extreme lattice spacings. Key value offsets occur when maxima, minima, inflection points, or other landmarks of a value's profile are shifted axially from where they occur at rest lattice spacings. Key value offsets are reflected in phenomena such as the axial offset at which a powerstroke will occur becoming right shifted at higher lattice spacings for the 2sXB. In addition to these lattice spacing dependencies, we examine the ability of the 4sXB and the 2sXB to model the radial component of the force produced during the powerstroke.

Key points of transition rates and energies vary with lattice spacing For both crossbridges modeled here, the axial offset and baselines that characterize their energy and transition rate curves vary with lattice spacing. The changing axial offset of the energy and probability distributions is visible in Figure 5 as a diagonal component to most of the shown contour lines. An example of this change in axial offset is visible in subfigures 5a and 5b where the lowest energy point that the 4sXB or the 2sXB may reach at a lattice spacing of 32 nm is more than three nm further from the crossbridge's thick filament attachment point than the lowest energy point reachable at a lattice spacing of 42 nm. Similar phenomena can be seen in the binding rate and detachment rate contours shown in subfigures 5c, 5d, 5e, 5f, 5g, and 5h. The powerstroke rates shown in subfigures 5e and 5h also have a landmark point that is dependent on the lattice spacing, but are slightly different in that landmark is the inflection point of the transition probability rather than a maximum or minimum.

Magnitude of transition rates and energies vary with lattice spacing Change in the baseline of the of the energy or transition rates as lattice spacing changes is separate from the altered axial offset of the rates and energies described above. In all cases except that of the powerstroke rate we are dealing

with profiles that are parabolic with lattice spacing as well as axial offset. This means e.g. that the probability of binding at the most favorable axial offset is still less at either extreme of lattice spacing than it will be at a rest lattice spacing. Likewise, any crossbridge that does manage to find its way to a force generating state will not remain in that state for long at the extremes of lattice spacing. The powerstroke rates shown in subfigures 5e and 5h are again slightly different, and do not vary in magnitude with lattice spacing. The powerstroke rates are dependent on the difference between two parabolic energy profiles, that of their respective crossbridges in the loosely bound state and in the strongly bound state. All other contours shown depend on only one parabolic component, the free energy of the unbound crossbridge being fixed at zero.

Kinetics at rest lattice spacings are similar to previous efforts The the free energy, binding rates, powerstroke rates and detachment rates of the 4sXB, 2sXB, and 1sXB are largely similar when viewed at a rest lattice spacing of 37 nm, as seen in Figure 5. The 1sXB values used here are calculated using the methods which produced Figure 10 in Tanner et al. (5). This serves as a confirmation that the modifications which generalize the kinetics to two and higher dimensions do not strip away too many of the properties present in prior 1sXB models. Subfigure 5b shows that using a thermally forced diffusion step in the calculation of attachment rates creates a very similar profile to that seen with non-physical methods. The largest departure from previous kinetics occurs in the detachment rates, where the prior kinetics were least based on the energy of the crossbridge, and thus where the greatest departures were needed to produce a generalized system that functions for all spring-based crossbridges.

Radial forces are on same order as axial forces, dependent on lattice spacing and axial offset The forces exerted by a 4sXB or 2sXB, when moved from its rest position to an axial offset, will have a radial component at all lattice spacings as shown in figure 5. Examining the force vectors in figure 5, produced by he compression or expansion caused when a crossbridge head is moved from its position of lowest energy, reveals that they are often off the horizontal by 45° or more. Such a deviation from purely horizontal, or axially aligned, force vectors indicates that the radial forces present are on the same order of magnitude as the axial forces. The size of these radial forces also appears to be more dependent on lattice spacing than that of the same crossbridge's axial forces. This increased dependence, due to changes in lattice spacing being changes in the radial direction, results in larger compressive force accompanying larger lattice spacings on a per crossbridge level.

Axial force offset, but not magnitude, varies with lattice spacing The axial force, which is the force directed in the direction of muscle shortening when

mapped to an intact system, varies less with lattice spacing than does radial force, as shown in figure 5. Similar to the energy levels above in figure 5, the baseline of the axial force changes little over the various lattice spacings examined. However, the axial offset producing the least force in the axial direction at a given lattice spacing does shift by several nm over the examined lattice spacings. Thus increased or decreased axial force produced by a single modeled crossbridge at altered lattice spacings is due more to changes in resting position than overall elevated levels of strain in the crossbridge's constituent springs.

4 Discussion

Strain and force generation at the level of a single crossbridge depend on lattice spacing Lattice spacing greatly alters the kinetic landscape to which individual multi-spring crossbridges are subject. Complex, and not entirely easy to visualize interactions occur between different kinetic rates with varying lattice spacing. A single example of this is that, for the 2sXB, the small lattice spacing axial offsets that are most likely to bind are increasingly less likely to quickly complete a powerstroke, due to the shift in the powerstroke rate's inflection point. In addition to lattice spacing altering the interactions between kinetic rates, radial forces are found to be present at levels which often equal axial forces. Multiple spring crossbridges open new doors to explore the relationships between kinetics, lattice spacing, radial force and axial force.

Simplicity of the 2sXB may be desirable While the 2sXB does not exactly mirror the behaviors of the 4sXB, it does resemble them in most ways (as seen in figures 5, 5 and 5) and may be the best option for further use in spatially explicit models due to its low computational requirements. As mentioned in the methods section, whenever the head of the 4sXB is moved the position of the middle torsional spring, roughly equivalent to the convertor domain, must be found through an iterative technique. This imposes a computation cost that is small for a single crossbridge, but which make longer duration multifilament simulations untenable. These problems do not exist for the 2sXB which requires no such step. As the kinetics and force of the 2sXB system resemble those of the 4sXB system in most instances, with the exceptions of their differing lattice spacing dependencies of the powerstroke rate and precise force orientation at some of the more extreme offsets, it may prove to be a useful model system.

Increased fidelity to known structure and mechanisms The multiple spring crossbridges both have a far greater ability than single spring crossbridges to replicate the defining characteristics of muscle myosin structure and the lever arm mechanism of force generation. The 2sXB and the 4sXB both generate force

through the changing of the rest angle of a torsional spring attached to a lever arm. This is closely analogous to the lever arm mechanism as it is understood and stands in contrast to the mechanism by which a single spring crossbridge replicates the powerstroke (6). The single spring crossbridge generates its force with an offset of the myosin head can also be thought of as the spring representing the crossbridge having a different rest length in the unbound state and the loosely bound state than it does in the tightly bound state. This offset or altered rest length is what determines the stroke distance of the single spring crossbridge and estimates of it have varied from as little as 1 nm to as large as 10 nm (needs citation). By treating the crossbridge as several components instead of a single spring we are able to base input parameters on values that can be referenced to existing crystallography structures.

Step size varies with lattice spacing for a two spring crossbridge Inherent in the geometry of the 2sXB and the 4sXB is a change in step size with a change in lattice spacing. Step size at a given lattice spacing is defined as the axial distance a myosin head moves between pre- and post-powerstroke angles if unconstrained in the axial direction and allowed to settle into the position which minimizes the energy of the crossbridge. These changes in step size occur because the angle which a given axial movement subtends increases with decreasing lattice spacings. This scenario also depends on the linear spring between the myosin's pivot point and the thin filament changing in length to accommodate differing lattice spacings. The single linear spring of the 2sXB is the only means by which the 2sXB may span the distance from the single torsional spring to the thin filament and thus must change with lattice spacing. However, the 4sXB is also possessed of the torsional and linear springs which are more proximal to the thick filament. These additional springs also adjust with lattice spacing, allowing the location of the 4sXB's pivot point to alter so that the difference in step size with changes in lattice spacing is smaller, although still present. This is yet another factor that may alter the force generated at different lattice spacings, increasing the strain and probability of detachment shortly after completing the powerstroke at larger lattice spacings.

Modeled radial forces are too large to ignore Simulated radial forces for both the 2sXB and the 4sXB were of the same order as the axial forces being produced. Inclusion of these forces in future modeling efforts presents an opportunity to examine an type of interaction ignored by previous spatially explicit models. Experimental evidence for the existence of strong radial forces during contraction is provided, at the level of muscle fibers, by observations of lattice spacings during redevelopment of tension in Cecchi et al. (10). Spatially explicit explorations of how these forces are transmitted throughout the lattice, or what restoring force prevents the creation of an overly disordered lattice where radial forces kink thick and thin filaments out of their axial paths are

possible with either presented crossbridge.

5 Figures

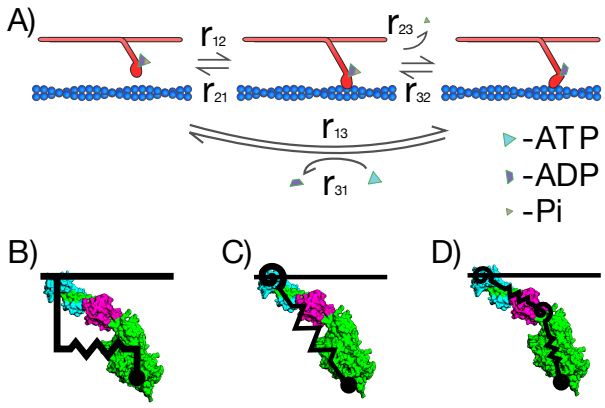

Figure 1: **Kinetic scheme and crossbridge types under investigation.** The three state kinetic system used both here and in prior models is shown in subfigure a). The three states represented are an unbound state (1), a loosely bound state (2), and a strongly bound state (3). The binding rate ($r_{1,2}$), strong transition rate ($r_{2,3}$), and unbinding rate ($r_{3,1}$) at a given location are functions of the energy stored in the springs representing the crossbridge, if the crossbridge head is moved to that location. The reverse rates ($r_{2,1}$, $r_{3,2}$, and $r_{1,3}$) are all functions of the forward transition rates. Subfigures b), c), and d) show the various spring based representations of the crossbridge. Subfigure b) shows the single spring crossbridge representation used in models since (1). Subfigure c) shows the two spring system, consisting of a torsional/angular spring and a linear spring, that we propose to allow the modeling of radial forces. Finally, subfigure d) shows the four spring system using two torsional and two linear springs which we also compare to the single and dual spring crossbridges.

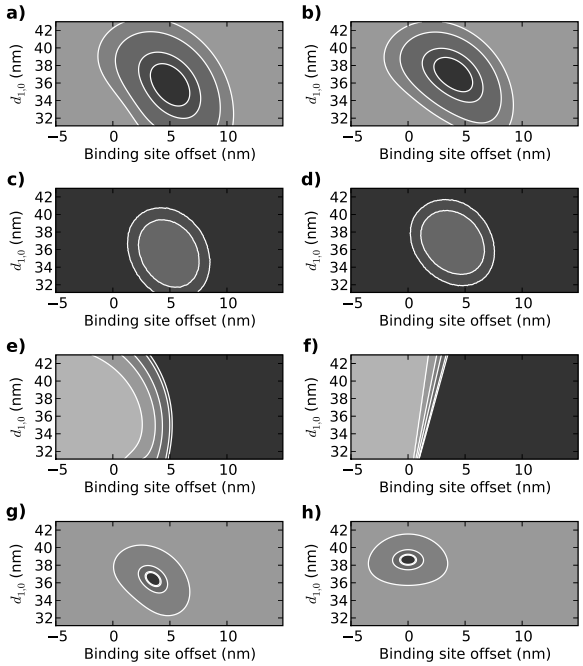

Figure 2: **Energy and kinetics of the 4sXB and 2sXB systems at varying axial offsets and lattice spacings.** The free energy of the four spring crossbridge at various lattice spacings (represented along the y-axis), with the head stretched to an axial offset from the point where it attaches to the thick filament (zero on the x-axis) is depicted in a). Simmilarly, the free energy of the two spring crossbridge is represented in b). The subfigures c) and d) show $r_{1,2}$, the probability that the four and two spring crossbridges will transition from an unbound state to a bound state, and the dependence of this transition on both the axial offset of the open binding site from the myosin thick filament attachment site and the lattice spacing $d_{1,0}$ which is a function of the distance between the binding site and the thick filament attachment point of the myosin head. Subfigure c) depicts this probability for the four spring crossbridge as a two dimensional contour with the same axes as a) while subfigure d) depicts the transition probabilities for the two spring crossbridge. Subfigures e) and f) show $r_{2,3}$, the probability of transition from a weakly bound state to a strongly bound state, for the same crossbridges, with the same axes and scales as c) and d) show $r_{1,2}$. Subfigures g) and h) show $r_{3,1}$, the probability of unbinding from a strongly bound state, for the same crossbridges, with the same axes and scales as c) and d) show $r_{1,2}$. The reverse rates, $r_{2,1}$, $r_{3,2}$, and $r_{1,3}$ may be back-calculated from the forward rates via the method described in (5).

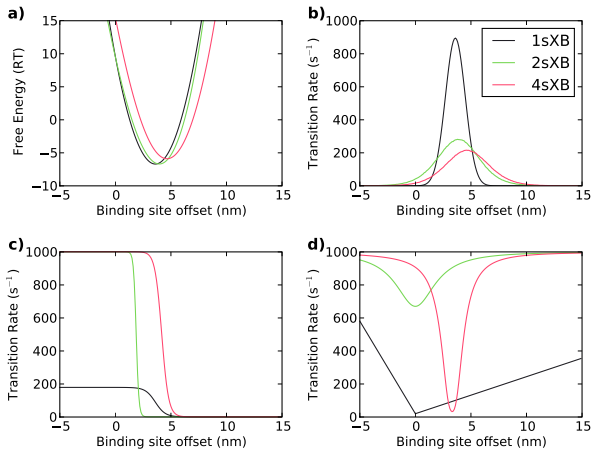

Figure 3: **Energy and kinetics of the four, two and single spring crossbridges at the resting lattice spacing.** Comparison of traditional single spring crossbridge properties to those of the two spring crossbridge at resting lattice spacing.

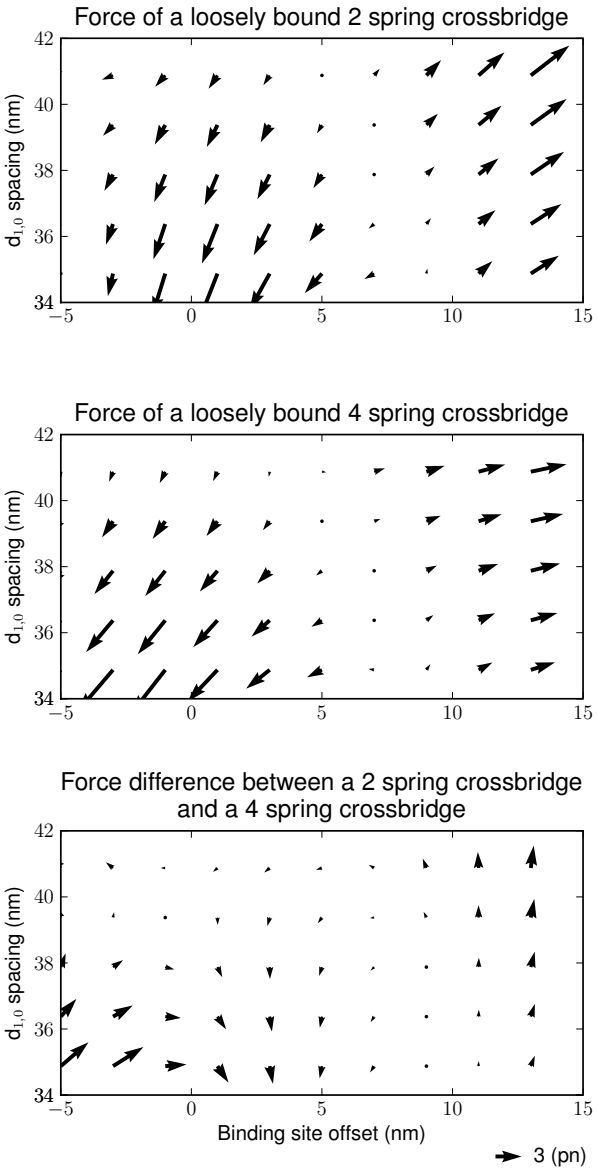

Figure 4: **Force vectors of the two and four spring crossbridges, and the differences between.**

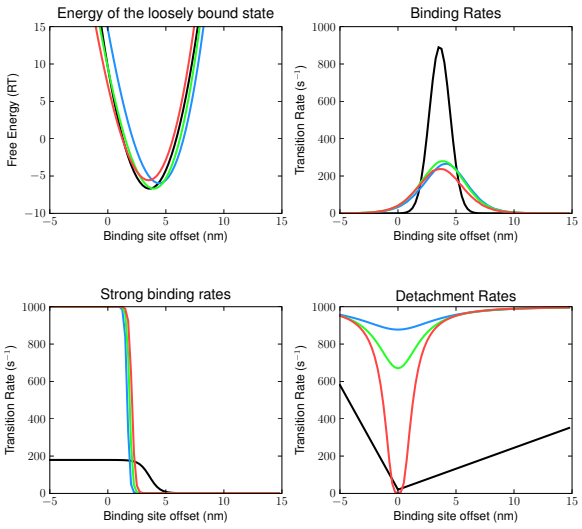

Figure 5: Comparison of traditional single spring crossbridge properties to those of the two spring crossbridge at resting lattice spacing.

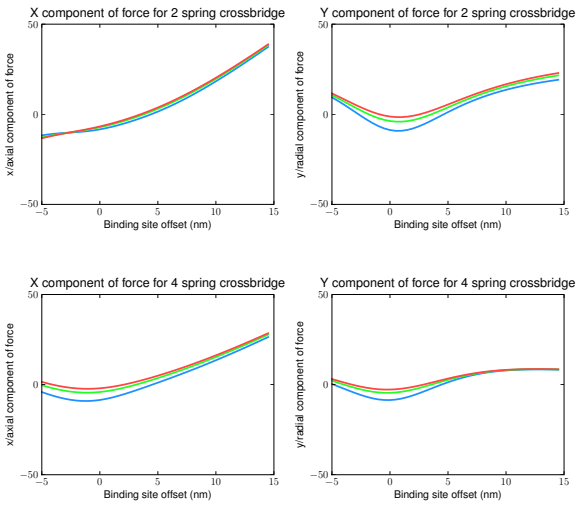

Figure 6: Separated axial and radial components of force exerted by the two spring crossbridge at several lattice spacings.

References

[1] Huxley, A., 1957. Muscle structure and theories of contraction. *Progress in biophysics and biophysical chemistry*

[2] Pate, E., and R. Cooke, 1989. A model of crossbridge action: the effects of ATP, ADP and Pi. *J Muscle Res Cell Motil*

[3] Daniel, T., A. Trimble, and P. B. Chase, 1998. Compliant realignment of binding sites in muscle: transient behavior and mechanical tuning.

[4] Chase, P. B., J. M. Macpherson, and T. L. Daniel, 2004. A spatially explicit nanomechanical model of the half-sarcomere: myofilament compliance affects Ca(2+)-activation. *Annals of biomedical engineering*

[5] Tanner, B. C. W., T. L. Daniel, and M. Regnier, 2007. Sarcomere lattice geometry influences cooperative myosin binding in muscle. *PLoS Comput Biol*

[6] Houdusse, A., and H. L. Sweeney, 2001. Myosin motors: missing structures and hidden springs. *Curr Opin Struct Biol*

[7] Schoenberg, M., 1980. Geometrical factors influencing muscle force development. I. The effect of filament spacing ....

[8] Schoenberg, M., 1980. Geometrical factors influencing muscle force development. II. Radial forces.

[9] Houdusse, A., A. G. Szent-Gyorgyi, and C. Cohen, 2000. Three conformational states of scallop myosin S1. *Proc Natl Acad Sci USA*

[10] Cecchi, G., M. A. Bagni, P. J. Griffiths, C. C. Ashley, and Y. Maeda, 1990. Detection of radial crossbridge force by lattice spacing changes in intact single muscle fibers. *Science*